Conference Proceedings

EuroSun 2016
Palma de Mallorca (Spain), 11 – 14 October 2016

The influence of Sahara dust particles in the direct normal irradiance estimation through a total sky camera

Joaquín Alonso-Montesinos[1, 2], Javier Barbero[1], Gabriel López[3], Jesús Ballestrín[4], Jesús Polo[5], Aitor Marzo[6, 7] and Francisco Javier Batlles[1, 2]

[1] Department of Chemistry and Physics, University of Almería, 04120 Almería, Spain

[2] CIESOL, Joint Centre University of Almería-CIEMAT, 04120 Almería, Spain

[3] Department of Electrical and Thermal Engineering, Design and Projects, University of Huelva, 21004, Huelva, Spain

[4] Concentrating Solar System Unit (Plataforma Solar de Almería, CIEMAT), 04200 Almería, Spain

[5] Photovoltaic Solar Energy Unit (Renewable Energy Division, CIEMAT), 28040 Madrid, Spain

[6]Antofagasta Energy Development Center (CDEA), 02800 Antofagasta, Chile

[7] Solar Energy Research Center (SERC-Chile), Santiago (Chile)

Abstract

To properly operate Central Tower Solar Power (CTSP) plants, collection systems must work under appropriate weather conditions. Therefore, knowing the state of the atmosphere, and more specifically the level of incident radiation, is a very valuable information for the operation, to adapt the system for electricity production to atmospheric conditions. Sky cameras have emerged as terrestrial point technologies that can observe the changes produced in short-time intervals. In this work, we have estimated Direct Normal Irradiance (DNI) using a total sky camera (TSI-880 model) under high dust load to study its effect in the DNI estimation, for next compare the results with a cloudless day without these attenuator particles. Furthermore, a CL-51 Vaisala ceilometer was used to identify the presence of this dust concentration in the atmosphere.

Keywords: *Solar radiation estimation, Atmospheric attenuation, Central tower solar power plants, Sky camera, LIDAR*

1. Introduction

The great majority of CTSP plants are in areas with low or medium probability of occurrence of clouds, but high probability of occurrence of episodes of high concentrations of aerosols or dust intrusion. That is why it is necessary to include both factors of a correct evaluation and prediction of the values of direct radiation in the receiver of the tower.

Sky cameras have been used to characterize the atmosphere from a terrestrial point. Its technology makes can be installed in any geographical location, providing a hemispheric view of the sky in real time. Subsequently, many researchers have used these cameras for cloud detection (Alonso et al., 2014) and solar irradiance estimation (Alonso-Montesinos and Batlles, 2015). In that case, atmospheric constituents play also an important role in the radiation attenuation and must be take into account in the solar irradiance estimation.

On 22nd February 2016, an intense episode of Sahara dust intrusion took place in almost all of the Iberian Peninsula, reducing visibility drastically and producing a remarkable dust deposition. In the southeast, Almería was particularly affected by the event (Alonso-Montesinos et al. 2016). Having a sky free of clouds, the DNI estimation was carried out, obtaining a results very distant than in a normal cloudless sky.

doi:10.18086/eurosun.2016.09.05 Available at http://proceedings.ises.org

Therefore, in this work, we present the influence of the concentration of dust particles in the DNI estimation using a total sky camera (TSI-880 model). To ensure the presence of this dust deposition in the lower atmosphere layers, LIDAR data were used from a CL-51 Vaisala ceilometer, obtaining different atmospheric parameters for the days studied.

2. Data

Radiation data were obtained from a radiometric station placed at CIESOL at the University of Almería, Spain (36.8ºN, 2.4ºW, at sea level), at the same time that total sky images (from TSI-880 sky camera) have also collected. The hemispheric vision was represented in JPEG (joint photographic expert group) images, with a 352x288 pixel-image resolution. Furthermore, CL51 Vailasa data were used. Fig. 1 shows the instrumentation in the rooftop of the CIESOL building.

Fig. 1: Total sky camera, TSI-880 model and CL51 Vaisala ceilometer placed in the rooftop of the CIESOL building at the University of Almería

3. Methodology and results

In this section, a particular episode occurred in the southeast of Spain is presented where dust particles appeared over Almería, provoking a decrease in the Direct Normal Irradiance (DNI). Therefore, a case study was performed for estimating DNI using a total sky camera under this special situation. The estimations for this turbid day were compared with the estimations for a clear day, obtaining representative conclusions. Furthermore, CL51 Vaisala ceilometer data were used to contrast the causes of the DNI decreasing.

The importance of this study comes from the special interest of CTSP plants, which need to measure the DNI attenuated in the lower layers of the atmosphere. Therefore, one of the main goal of these plants is to model the irradiance losses between the heliostats and the receiver placed at the top of the tower.

3.1 Turbid day vs clear day

As the idea of this paper is to determine the influence of dust particles in the estimation of DNI with total sky cameras, two contrasted days were selected. The first day was conditioned by a high concentration of Saharan dust particles in the atmosphere (22nd February 2016). For the second day, we tried to choose a clear day in the same date but in other years, obtaining it on 22nd February 2012. Fig. 2 shows the difference of DNI measurements for both days:

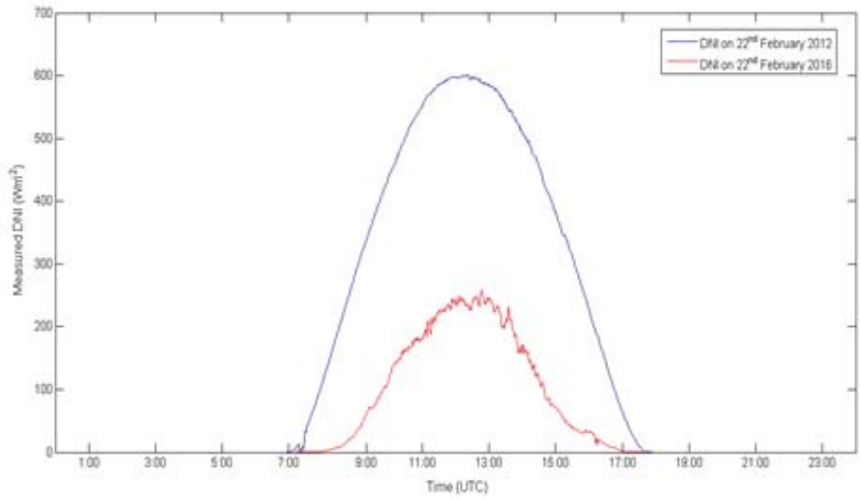

Fig. 2: Representation of measured DNI curves for the days 22nd February 2012 and 22nd February 2016

As seen, the DNI measured for the two days presented an important difference along the day. This difference was also captured by the total sky camera where the digital image levels were also very different. Fig. 3 shows the difference between the two sky camera images:

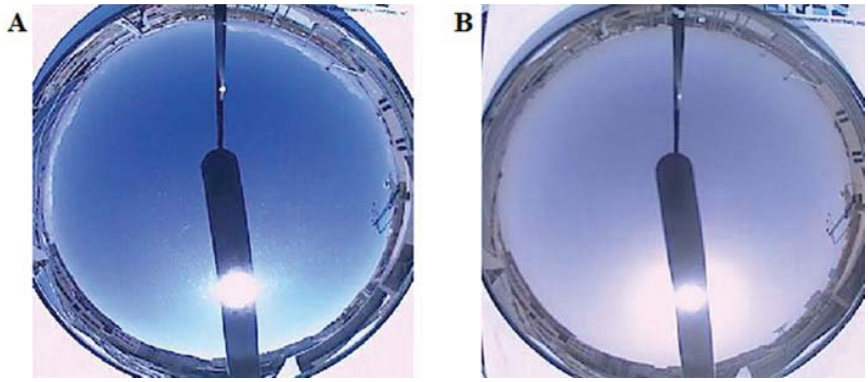

Fig. 3: Sky representation using a TSI-880 sky camera. The image A represents the sky on 22nd February 2012 at 12:00 Universal Coordinated Time (UTC), and image B on 22nd February 2016 at 12:00 UTC.

In the previous images, the blue sky presents a different appearance: in the picture A the sky appears in a more intense blue; whereas in the picture B, the sky appears with another blue tone (cloudier). Having this difference, the objective was to study the influence of the dust presence in the DNI estimation. Subsequently, the idea was to see how the atmosphere was composed in the lower layers with the CL51 Vaisala ceilometer. As Vaisala was installed in the CIESOL building in 2014, there was not data available from 2012. Then, a day with similar DNI was searched, finding 1st March 2016 like the most suitable. Figure 4 represents the DNI curves for 22nd February 2012 and 1st March 2016 to see that the DNI values had a similar trend in the two days:

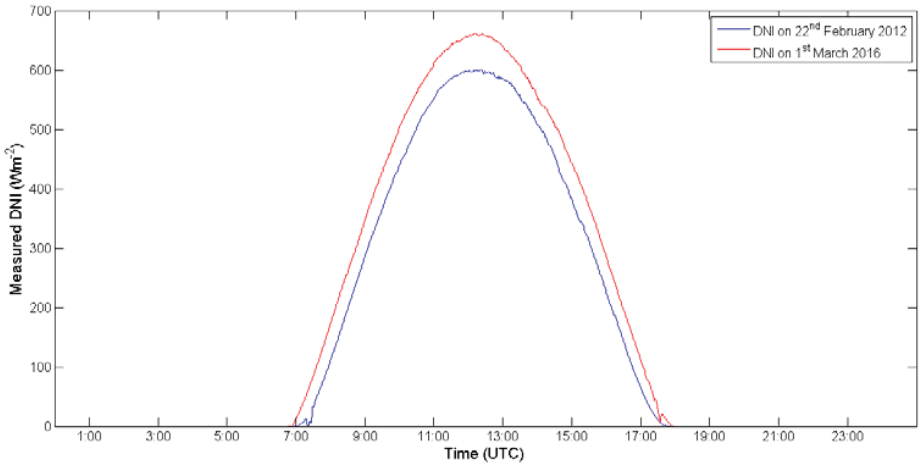

Fig. 4: Representation of measured DNI curves for the days 22nd February 2012 and 1st March 2016

The DNI on 1st March presented higher values than 22nd February, indicating a clearer day. Therefore, the first day of March was selected like the clear sky for comparing with 22nd February 2016 (dust episode). Figure 5 shows an image for the selected day, where blue sky does no present any perturbation in the atmosphere due to dust particles apparently.

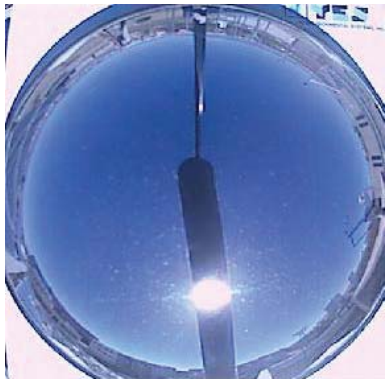

Fig. 5: Image from TSI-880 sky camera on 1st March 2016 at 12:00 (UTC)

3.2 DNI estimation using a total sky camera

According to methodology presented in Alonso-Montesinos and Batlles, (2015) and Alonso-Montesinos et al., (2015), the DNI was estimated using TSI-880 sky images for the two studied days: 22nd February 2016 and 1st March 2016. The first one presented the concentration of Sahara dust particles; whereas the second one was a cloudless sky where dust particles do not appear.

Digital image levels are used to estimate a DNI value. For DNI, not all pixels are processed; only pixels in the sun area. As the sun area has not always the same size, a radius which covers the solar area is obtained in function of the solar altitude angle (α), following the next expression:

$$Radius = -0.9646\,\alpha + 99.2986 \qquad \text{(eq. 1)}$$

Figure 6 represents the solar area detected for a cloudless moment, where the red circle represents the sun area to estimate the DNI.

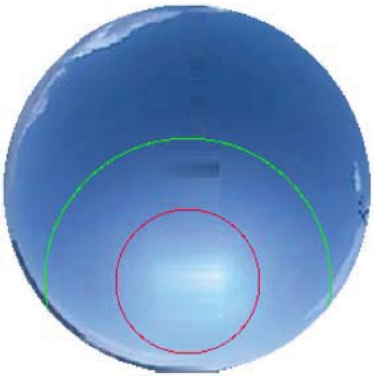

Fig. 6: Image from TSI-880 sky camera, where different areas are established to do the estimation of radiation.

After that, using digital image level correlations and the solar altitude angle, each pixel belonging to the red circle acquires a DNI value following the methodology described in the previous cites. Finally, the mean value of the total pixel estimations represents the DNI.

From sunrise to sunset, images from the sky cam were processed every minute. For all results, different parameters were obtained: RMSE given by Eq. (2) and expressed in (Wm^{-2}); nRMSE given by Eq. (3) in (%); MBE given by Eq. (4) and expressed in (Wm^{-2}); nMBE given by Eq. (5) in (%) and R given by Eq. (6) (dimensionless):

$$RMSE = \sqrt{\frac{1}{N}\sum_{i=1}^{N}(DNI_{est} - DNI_{mea})^2} \quad \text{(eq 2)}$$

$$nRMSE = \left[\frac{RMSE}{DNI_{max} - DNI_{min}}\right] 100 \quad \text{(eq 3)}$$

$$MBE = \frac{1}{N}\sum_{i=1}^{N}(DNI_{est} - DNI_{mea}) \quad \text{(eq 4)}$$

$$nMBE = \left[\frac{MBE}{DNI_{max} - DNI_{min}}\right] 100 \quad \text{(eq 5)}$$

$$R = \frac{\sigma_{DNI_{est}DNI_{mea}}}{\sigma_{DNI_{est}}} \quad \text{(eq 6)}$$

where DNI_{est} is the DNI estimated, DNI_{mea} is the DNI measured, DNI_{max} is the maximum observed DNI value, DNI_{min} is the minimum DNI value, $\sigma_{DNI_{est}DNI_{mea}}$ is the covariance of the two input data sets (the estimated and measured radiations), $\sigma_{DNI_{est}}$ is the standard DNI_{est} deviation and $\sigma_{DNI_{mea}}$ is the standard DNI_{mea} deviation. Tab. 1 shows the numerical results:

Tab. 1: DNI estimation results for the two day analyzed: 22nd February 2016 (turbid day) and 1st March 2016 (clear day).

Day	RMSE (Wm^{-2})	nRMSE (%)	MBE (Wm^{-2})	nMBE (%)	R
22nd February 2016	192.87	50.36	-141.35	-36.91	0.27
1st March 2016	137.68	16.17	50.13	5.89	0.95

As seen, the results on February presented an nRMSE value higher than on March in a value of 30%. Furthermore, the nMBE presented a high difference; on February, the DNI was underestimated, with a mean value of -37%; whereas on March, the value was lower than 6%. The underestimation was consequence of the classification of pixels. In the February's case, the pixels were classified like overcast due to the digital image level of the pixels that belong to the red circle, and therefore, the DNI estimation was done for an overcast day. As seen, the DNI estimation model is only based on the image digital values without considering atmospheric measurements. By this reason, in a free cloud day, the appearing of dust situations provokes that the model presents results very far than for typical cloudless skies. Therefore, CL51 Vaisala ceilometer data were used to see the behavior of the atmosphere, having another tool which could improve the solar radiation estimation.

3.3 Determination of atmospheric factors using a LIDAR ceilometer

CL51 Vaisala ceilometer with LIDAR technology, provides atmospheric information (from 0 to 4 kilometers) related to aerosol presence and visibility, and gives indirect information to calculate some atmospheric factors. Therefore, with the data collected, it is possible to identify the main attenuation factors helping to improve the solar radiation estimation models.

In the case of study of this paper, the profiles for the two analyzed days were studied, and the complete distributions are presented in Fig. 7, where it is shown the evolution along the whole day of the attenuated backscatter intensity (ABI) profiles from ground up to 4 km:

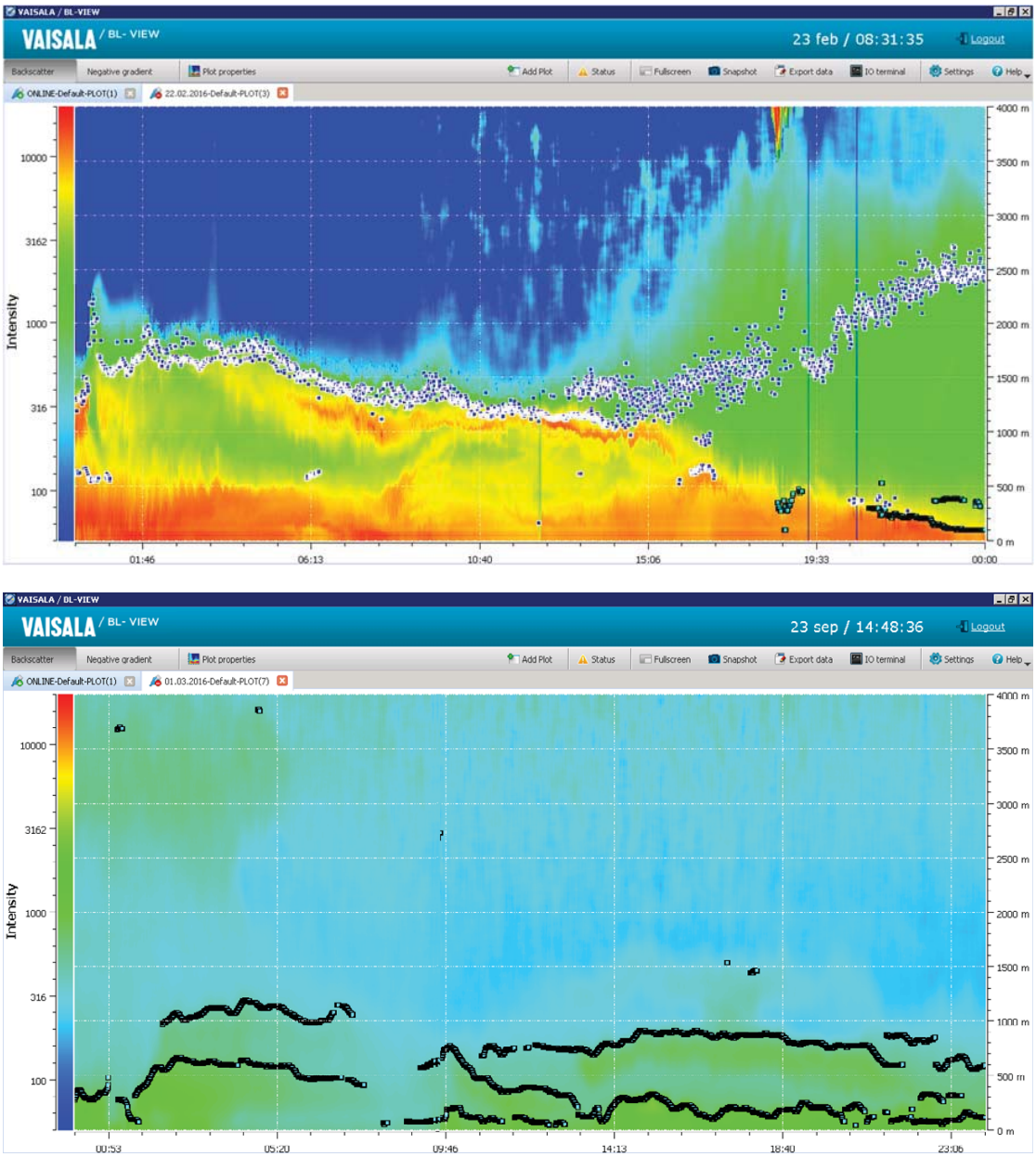

Fig. 7: CL51 Vaisala ceilometer profiles: the upper image represents the profiles on 22nd February 2016, and the other one represents the profiles on 1st March 2016

In this figure, important information is extracted for the two days. In the case of 22nd February, the most relevant data are presented below:
A nearly static dust layer 500 meters thick appears. With the sunrise, the surface temperature rises and this layer expands up to the boundary layer. Another thin layer, in the upper limit of the residual boundary layer appears floating on the boundary layer. From 16:00 UTC to the end of the day, the two layers precipitate progressively, appearing an expanding region of intermediate Attenuated Backscatter Intensity (ABI) values (in green) reaching up to 4 km in altitude.
For the analyzed case on 1st March, the atmosphere presents clear profiles (low intensity values) along the day. Perhaps, from 14:00 hours to midnight, a higher concentration of particles appears in the lower atmospheric layers (from 0 to 250 meters) but in a lower degree than on 22nd February. However, this first day of March can be considered like a very clear day.

As seen, the most important successes occurs in the lower layers (being more representative from 0 to 250 meters, approximately). Taking into account the interest of CTSP plants in the study of the sky conditions in these lower atmospheric layers to quantify the DNI losses between the heliostats and the receiver placed at the top of the central tower, these layer are analyzed. Furthermore, the first 250 meters are enough to measure the losses, covering the higher towers built in the plants.

Therefore, the inclusion of LIDAR information in DNI estimation models can improve the accuracy of that. For this reason, different atmospheric factors have been obtained from LIDAR measurements. Subsequently, ABI has been analyzed with the aim to determine the Meteorological Optical Range (MOR) and the Aerosol Optical Thickness (AOT) from 0 to 250 meters. Concretely, the profiles were obtained at midday (12:00 UTC) for an average time of 20 minutes in the two selected days.
The extinction coefficient (K_{ext}) is obtained solving the ceilometer equation, for a given profile, taking a particular Lidar Ratio (LR). The LR is a variable which depends on the aerosols and the water vapor, being 33 $(Wm)^{-1}$ for a cloudless sky by the manufacturer. Figure 8 represents the K_{ext} coefficient on 22nd February.

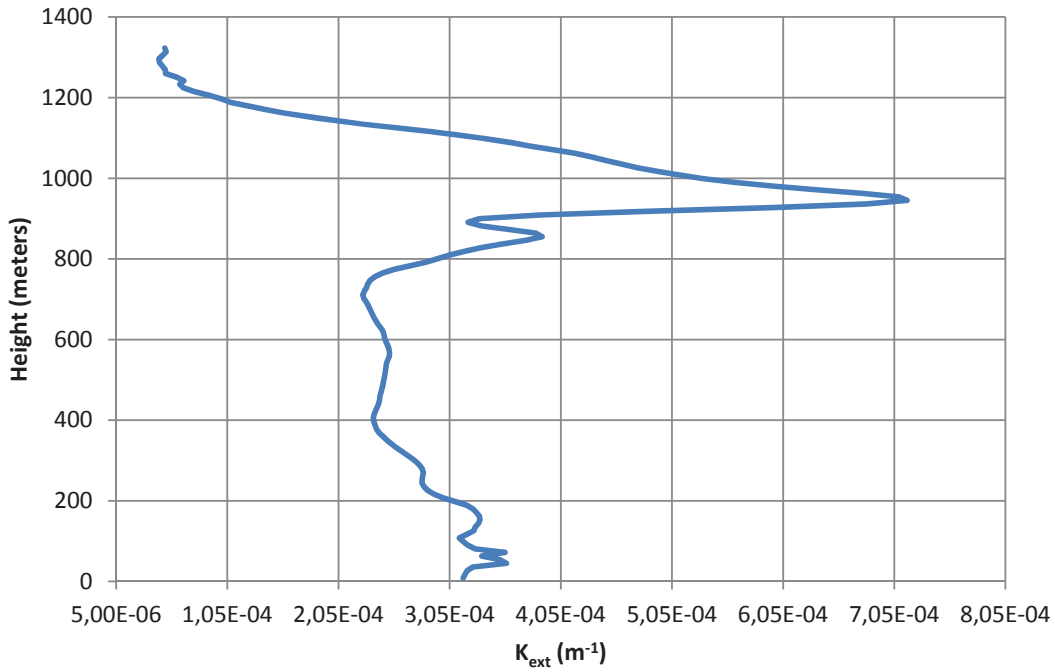

Fig. 8: K_{ext} profile obtained from CL51 Vaisala ceilometer on 22nd February 2016 at 12:00 UTC

Analyzing the graph, the coefficient shows similar values in the lower atmospheric layers (until 500-600 meters approximately), having a high dispersion from 800 to 1300 meters. It means that the atmospheric composition was homogenous in the low layers with a K_{ext} coefficient value between $2.5E^{-04}$ and $3.5E^{-04}$; and next, the homogeneity changed significantly. For comparing this day with the clear studied day, Figure 9 shows the K_{ext} profile on 1st March 2016:

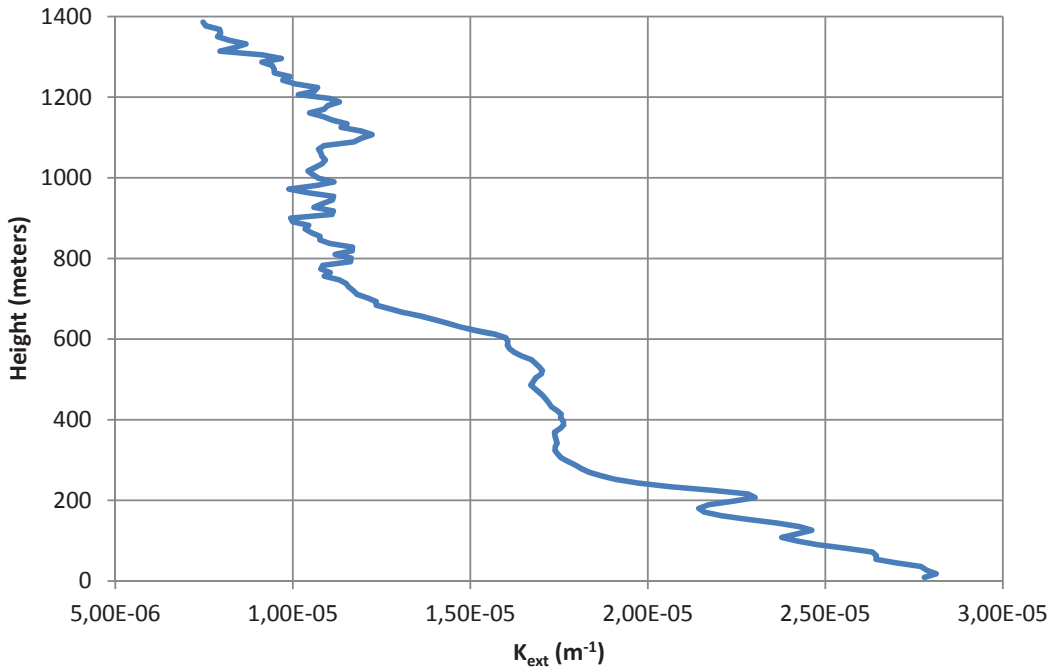

Fig. 9: K_{ext} profile obtained from CL51 Vaisala ceilometer on 1st March 2016 at 12:00 UTC

In this case, the K_{ext} values were lower than the values registered on February. For the first 250 meters, the K_{ext} values presented a decrease, reaching values between $2.8E^{-05}$ for 9 meters and $1.9E^{-05}$ for 250 meters.

The MOR (expressed in meters) was also calculated following the next equation:

$$MOR = \frac{3}{K_{ext}} \qquad \text{(eq 7)}$$

Together with the averaged K_{ext} values and the MOR parameter, the AOT was obtained integrating the K_{ext} into the first 250 meters. As the CL51 ceilometer profiles are retrieved every 9 meters, we integrated the coefficient from ground to 252 meters (multiple of 9). Table 2 shows the summary of variables for the two days:

Tab. 2: Atmospheric variables obtained from CL51 Vaisala LIDAR ceilometer from ground to 252 meters

Day	K_{ext} (m^{-1})	MOR (Km)	AOT (910nm)
22nd February 2016	$3.19E^{-04}$	9.40	$8.04E^{-02}$
1st March 2016	$2.40E^{-05}$	125.00	$6.05E^{-03}$

The results show a significant difference between the two analyzed days: in the case of 22nd February, the K_{ext} coefficient was higher than on March, and consequently, the MOR was different too. In the case of February, the dust particles provoked that the MOR decreased until 10 Km approximately, whereas for the case of March, with a clean atmosphere, the MOR was higher than 120 Km. The AOT obtained at 910 nm was also lower under a clear sky, presenting a value of $8.04E^{-02}$ with the presence of dust particles, and $6.05E^{-03}$ for a very clear atmosphere in the lower layers.

Therefore, considering LIDAR measurement, the DNI estimation can be improved taking into account the attenuation coefficients in the processing of total sky images. The coefficients calculated can help to determine the optical properties of sky cam images depending on the contamination degree which appears in the digital image levels. With that, the interpretation of the pixel like cloudless or overcast is improved, and the consequent DNI estimation too.

4. Conclusions

In this work, a Sahara dust episode occurred the last 22nd February 2016 has been studied and compared with a totally clear day (1st March 2016) using a TSI-880 total sky camera and a CL51 Vaisala ceilometer with LIDAR technology.

The DNI was estimated using the TSI camera for the two studied days using the digital image levels. On 22nd February, where the intensity of dust particles was very high, the nRMSE value was higher than 50%, whereas the nMBE value presented an underestimation of 37%. The other day, 1st March 2016, presented an atmosphere free of dust particles, and the DNI estimation presented better results, where the nRMSE value was of 16% and the nMBE was lightly overestimated, with a value of 6%. In this case, the R coefficient presented also good values. Therefore, the results show that the nRMSE can differ in more than 30% under cloudless skies, if particular episodes, like the scenarios presented on February, appear.

LIDAR data from the CL51 Vaisala ceilometer have been used to obtain atmospheric parameters. K_{ext}, MOR and AOT were obtained for the turbid and for the clear day, showing a high difference. In the case of K_{ext} and AOT the values were lower in the clear day, and the MOR presented lower values in the turbid day.

As seen, dust particles have an important impact in the solar irradiance. Depending on the particle load, the attenuation of solar radiation can be more or less important. Theferore, the DNI estimation with sky cams can be improved using LIDAR data, where the atmospheric parameters are quantified, helping to identify the correct classification of pixels and, consequently, improving the solar irradiance estimations.

Acknowledgments

Financial support by the Education and Competitiveness Ministry of Spain, PRESOL project “Forecast of solar radiation at the receiver of a solar power tower” with references ‘ENE2014-59454-C3-1-R1, 2 and 3’. Also, the authors acknowledge the generous financial support provided by the Education Ministry of Chile Grant PMI ANT1201, the Fondecyt Project 3160190, as well as CONICYT/ FONDAP/ 15110019 "Solar Energy Research Center" SERC-Chile.

5. References

Alonso J., Batlles F. J., Ternero A., López G., 2014. Sky camera imagery processing based on a sky classification using radiometric data. Energy. 68, 599-608.

Alonso-Montesinos J., Batlles F. J., 2015. The use of a sky camera for solar radiation estimation based on digital image processing. Energy. 90, 377-386.

Alonso-Montesinos J., Batlles F. J., Portillo, C., 2015. Solar irradiance forecasting at one-minute intervals for different sky conditions using sky camera images. Energy Conversion and Management. 105, 1166-1177.

Alonso-Montesinos, J., Polo, J., López, G., Barbero, J., Bosch, J.L., Ballestrín, J., Batlles, F.J., 2016. Modelling clear sky DNI under extreme aerosol loading: the case of Saharan outbreak in south-east Spain. Proc. EuroSun2016 Conf., Palma de Mallorca (Spain).